Sharp contrasts between freshwater and marine microbial enzymatic capabilities, community composition, and DOM pools in a NE Greenland fjord

John Paul Balmonte ,[1*,a] Harald Hasler-Sheetal,[2] Ronnie N. Glud,[2,3] Thorbjørn J. Andersen,[4] Mikael K. Sejr,[5,6] Mathias Middelboe,[7] Andreas Teske,[1] Carol Arnosti[1]

[1]Department of Marine Sciences, The University of North Carolina at Chapel Hill, Chapel Hill, North Carolina
[2]Department of Biology, University of Southern Denmark, Odense, Denmark
[3]Department of Ocean and Environmental Sciences, Tokyo University of Marine Science and Technology, Tokyo, Japan
[4]Department of Geosciences and Natural Resources Management, Section for Geography, University of Copenhagen, Copenhagen, Denmark
[5]Arctic Research Center, Aarhus University, Aarhus, Denmark
[6]Department of Bioscience, Aarhus University, Silkeborg, Denmark
[7]Marine Biological Section, University of Copenhagen, Helsingør, Denmark

Abstract

Increasing glacial discharge can lower salinity and alter organic matter (OM) supply in fjords, but assessing the biogeochemical effects of enhanced freshwater fluxes requires understanding of microbial interactions with OM across salinity gradients. Here, we examined microbial enzymatic capabilities—in bulk waters (nonsize-fractionated) and on particles (≥ 1.6 μm)—to hydrolyze common OM constituents (peptides, glucose, polysaccharides) along a freshwater–marine continuum within Tyrolerfjord-Young Sound. Bulk peptidase activities were up to 15-fold higher in the fjord than in glacial rivers, whereas bulk glucosidase activities in rivers were twofold greater, despite fourfold lower cell counts. Particle-associated glucosidase activities showed similar trends by salinity, but particle-associated peptidase activities were up to fivefold higher—or, for several peptidases, only detectable—in the fjord. Bulk polysaccharide hydrolase activities also exhibited freshwater–marine contrasts: xylan hydrolysis rates were fivefold higher in rivers, while chondroitin hydrolysis rates were 30-fold greater in the fjord. Contrasting enzymatic patterns paralleled variations in bacterial community structure, with most robust compositional shifts in river-to-fjord transitions, signifying a taxonomic and genetic basis for functional differences in freshwater and marine waters. However, distinct dissolved organic matter (DOM) pools across the salinity gradient, as well as a positive relationship between several enzymatic activities and DOM compounds, indicate that DOM supply exerts a more proximate control on microbial activities. Thus, differing microbial enzymatic capabilities, community structure, and DOM composition—interwoven with salinity and water mass origins—suggest that increased meltwater may alter OM retention and processing in fjords, changing the pool of OM supplied to coastal Arctic microbial communities.

Heterotrophic microbial communities produce enzymes that catalyze organic matter (OM) transformations in environments spanning the land to ocean gradient; these microbial enzyme activities help determine the quantity and quality of OM exported to coastal systems. Along freshwater-to-ocean gradients, shifting physicochemical conditions exert pressure on microbial communities, including salinity-driven changes in community structure (Crump et al. 1999; Hewson and Fuhrman 2004; Fortunato and Crump 2015). Findings that compositionally distinct freshwater, estuarine, and marine microbes can differentially utilize the same OM pool (Fellman et al. 2010) suggest that differences in community members have consequences for carbon bioavailability and turnover. However, different levels of terrestrial and freshwater input along these aquatic continua are also manifested in varying ratios of autochthonous and allochthonous OM, which may consequently influence microbial activities (Paulsen et al. 2018). Thus, a critical ecological question with biogeochemical implications remains: to what extent do freshwater and marine

*Correspondence: jp.balmonte@gmail.com

Additional Supporting Information may be found in the online version of this article.

[a]Present address: Department of Ecology and Genetics/Limnology, Uppsala University, Uppsala, Sweden

microbial communities differ in their ability to initiate OM transformations, and are these distinct capabilities linked to variations in community composition, the external supply of OM, or both?

Characterizing biotic or abiotic control on microbial function along salinity gradients is especially relevant to forecast biogeochemical alterations in rapidly changing environments, in which salinity-related disturbances have been documented and continue to persist. For example, increased glacial discharge from the Greenland Ice Sheet, measured over a decade (2003–2015), has resulted in the freshening of subsurface waters in Tyrolerfjord-Young Sound in northeast Greenland (Sejr et al. 2017). However, the biogeochemical impacts of recent hydrological changes in this system—and, by extension, in similar fjord systems within the Arctic—remain elusive due to limited information about microbial communities and their activities. With few studies on microbial community structure in fjords (e.g., Zeng et al. 2009; Teske et al. 2011; Gutiérrez et al. 2015; Paulsen et al. 2017), on substrate preferences and enzymatic capabilities of freshwater and marine microbial taxa (Murrell et al. 1999; Stepanauskas et al. 1999; Eiler et al. 2014), and limited integrations between these parameters, the functional consequences of microbial community composition (Osterholz et al. 2016) across salinity gradients is little understood.

On the other hand, spatially distinct microbial activity and OM bioavailability patterns in river-to-fjord systems may be more proximately linked to differences in dissolved organic matter (DOM) supply (Lawson et al. 2014; Paulsen et al. 2017, 2018). Whereas riverine microbial communities in glacier-influenced Arctic rivers have access to allochthonous OM from glacial and terrestrial runoff (Hood and Scott 2008; Paulsen et al. 2017), coastal microbial assemblages have greater exposure to OM from autochthonous primary production, in addition to allochthonous OM from the heavily terrestrially influenced Arctic coastal water inflow (Amon et al. 2003). Autochthonous OM, especially nitrogen-rich components (Osterholz et al. 2014), can be mineralized rapidly by pelagic microbial communities, while allochthonous compounds may be relatively resistant to microbial remineralization (Paulsen et al. 2017). However, a considerable fraction of relict OM exported from glacial meltwater is, counterintuitively, efficiently degraded by coastal microbial communities (Hood et al. 2009; Lawson et al. 2014; Paulsen et al. 2017). Data from temperate and tropical systems suggest that along river-to-ocean transitions, freshwater microbial communities are attuned to the decomposition of carbohydrate-rich (Murrell et al. 1999; Cunha et al. 2000) and allochthonous OM (Ghai et al. 2011), while their marine counterparts may specialize in the breakdown of proteinaceous constituents. These patterns and processes underscore the biogeochemical consequences of freshwater and marine microbial interactions with varying OM pools, although they remain to be examined in high latitude coastal environments.

The role that particulate matter play in shaping microbial community composition and carbon remineralization also remains largely unidentified in high latitude fjords (Sperling et al. 2013; Osterholz et al. 2014; Jain et al. 2019). Studies from other aquatic environments demonstrate that particles can host bacterial communities with distinct composition (DeLong et al. 1993; Schmidt et al. 2016) and function (Fernandez-Gomez et al. 2013; D'Ambrosio et al. 2014) compared to their free-living counterparts. Furthermore, the composition of particle-associated bacterial communities differs across river-to-ocean gradients (Crump et al. 1999; Ortega-Retuerta et al. 2013; Bižić-Ionescu et al. 2015), although functional differences between particle-associated taxa in freshwater and marine environments are not well understood (Simon et al. 2014). Analyses of sinking particulate matter and sediments in fjords show evidence of both terrestrial and marine origins (Rysgaard and Sejr 2007; Bourgeois et al. 2016; Cui et al. 2017), suggesting that glacial discharge has the potential to shape microbial community structure in fjords through particle transport (Bhatia et al. 2013; Overeem et al. 2017; Jain et al. 2019). Indeed, estimates show that up to 90% of OM from the Greenland Ice Sheet is in particulate form (Bhatia et al. 2013). Moreover, high carbon burial rates in Arctic fjords (Glud et al. 1998; Smith et al. 2015; Sørensen et al. 2015) further imply that particulate matter evades complete remineralization in surface waters, and ultimately sinks to the bottom of fjords, sustaining benthic heterotrophs. A fraction of the OM that originated from the Greenland Ice Sheet may also be exported to the Arctic Ocean (Lawson et al. 2014). As microbially mediated particulate matter transformations in the water column greatly affect the quantity and quality of carbon sources available to benthic heterotrophs and coastal microbial communities, determining the identity and OM-degrading capabilities of particle-attached microbes across salinity gradients remains a priority.

In this study, we investigated the enzymatic capabilities of microbial communities to hydrolyze a range of organic substrates in Tyrolerfjord-Young Sound, a fjord in northeast Greenland in which a decrease in salinity has been observed (Sejr et al. 2017). We used a suite of structurally diverse peptide, glucose, and polysaccharide substrates, the hydrolytic enzymes for which have been found active in a range of freshwater (Murrell et al. 1999; Stepanauskas et al. 1999) and marine environments (Obayashi and Suzuki 2005; Arnosti et al. 2011; Balmonte et al. 2018; Balmonte et al. 2019). Moreover, these substrates and their constituent monomers comprise a substantial fraction of aquatic OM pool (Benner 2002). We hypothesized that bacterial community composition, enzymatic activity patterns, and DOM composition would vary strongly with salinity, a reflection of the different origins of water masses in these systems: glacial and terrestrial discharge transported to the fjord through rivers vs. coastal inflow of Arctic Ocean-derived water. Additionally, we hypothesized that particles discharged from glacial

rivers—a relatively unexplored source of microbial diversity in high latitude fjords—would host bacterial communities with distinct composition and range of enzymatic capabilities compared to those on autochthonous particles in the fjord. The extent to which freshwater vs. marine microbial communities differ in their ability to degrade and turnover specific compounds in the coastal Arctic has implications for future carbon processing in fjords, which are forecasted to continue experiencing salinity decreases (Sejr et al. 2017) and changes in OM pools (Hood and Scott 2008; Hood et al. 2015) owing to increased glacial melt.

Materials and methods

Site description and sample collection

Samples were collected during the summer melt season from 02 August 2015 to 17 August 2015 in Tyrolerfjord-Young Sound (Fig. 1). Surface-water samples were collected in 20-liter carboys from three main rivers with runoff from land-terminating glaciers that feed into Tyrolerfjord-Young Sound: Tyroler River (Tyro-R), Lerbugten River (Ler-R), and Zackenberg River (Zac-R); together, these sites will be referred to as "rivers." Tyro-R has the largest catchment area of the three rivers (Bendtsen et al. 2014), and runs from the Greenland Ice Sheet terminus to the fjord about 300 m downstream. The Tyro-R sampling site is about 250 m from the glacial terminus, and is estimated to be 100% glacial river. Ler-R is influenced by local glaciers (Paulsen et al. 2017), and runs from the glacial terminus to the fjord about 700 m downstream. Samples were collected in Ler-R about 600 m from the glacial terminus, and are also estimated to contain 100% glacial water. Zac-R has the most terrestrial and vegetative influence, receives input from two lakes, and is the largest river in the region. This river runs from the glacial terminus and drains into the fjord about 15 km downstream. Zac-R samples were collected about 400 m upstream of the fjord, and, while the vast majority of freshwater in August is from glaciers, the carbon content is strongly modified by the vegetation in the catchment (Paulsen et al. 2017). Surface (D1) and subsurface (D2) water samples were also collected at transition (T) sites where the rivers transition into the fjord: Tyro-T (ca. 1.4 km from Tyro-R), Ler-T (ca. 1.1 km from Ler-R), and Zac-T (ca. 1.4 km from Zac-R). Together, these locations are referred to as "river transition sites." Only the surface water at the river transition sites has a prominent freshwater signature, as waters below 20 m based on salinity are largely marine; thus, the surface waters at the river transition sites will be referred to as "river plumes." Surface and subsurface samples were also taken within the Young Sound (YS) fjord, as well as at

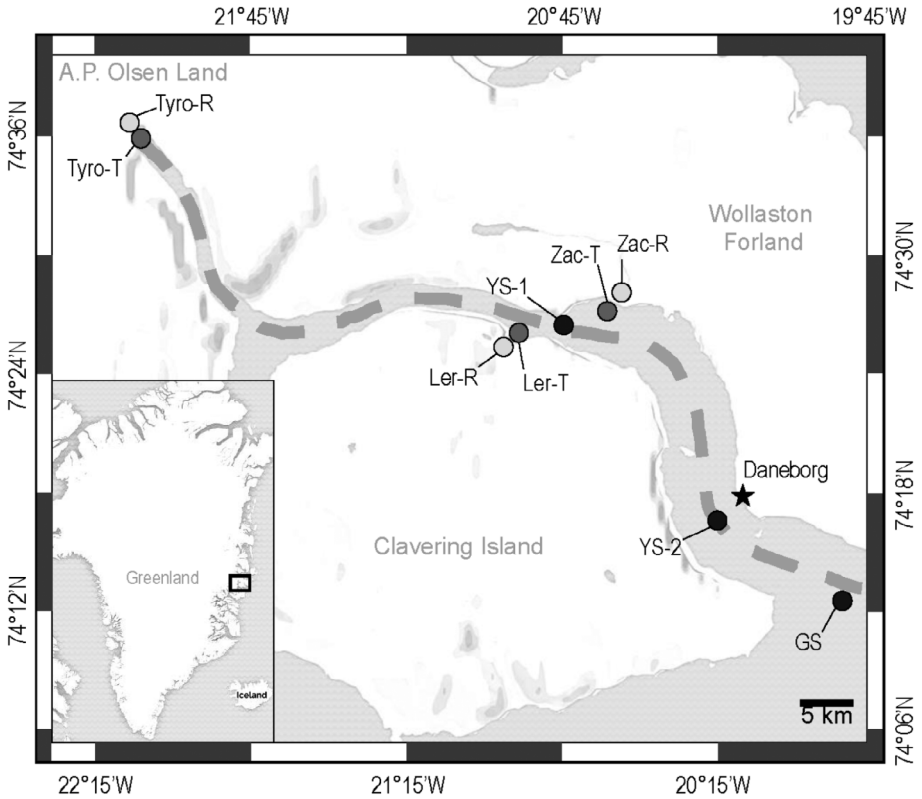

Fig. 1. Map of Tyrolerfjord-Young Sound. Sampling sites in the river (light gray), river transition sites (dark gray), and fjord and Greenland Sea (black) are denoted. Distances between river and river transition sites are included in "Materials and methods" section. "YS" and "GS" stand for Young Sound and Greenland Sea, respectively. The dashed line represents the basin of Tyrolerfjord-Young Sound. The land-based research station is located in Daneborg.

the mouth of the fjord close to the East Greenland Sea (GS): these stations are YS-1, YS-2, and GS, respectively, and collectively referred to as "fjord sites." Note also that four of the sites in this study (Tyro-T, YS-1, YS-2, and GS) are part of the Greenland Ecosystem Monitoring (GEM) *MarinBasis* program, and for clarity were renamed here. The original names of these stations as part of the *MarinBasis* program are as follows: Tyro_01 (Tyro-T), YS_3.18 (YS-1), YS_3.06 (YS-2), and GH_02 (GH).

Water samples from river transition sites and in the fjord were collected using Niskin bottles mounted with a conductivity, temperature, depth (CTD) sensor aboard the R/V *Aage V. Jensen*. As the volumes required for this work were large, water samples for all experiments could not be collected from the same Niskin bottle; however, water samples for the same site and depth were collected from the same CTD cast. Experiments were conducted at the land-based research station in Daneborg. Frozen samples collected as described below were transported back to the institutional laboratories for further processing.

Particle characteristics

Water samples were filtered through 0.45 μm Millipore mixed cellulose esters membrane filters, and the retained material was removed from the filters in plastic beakers placed in an ultrasonic bath. Samples were subsequently dispersed using a Bandelin Sonopuls HD2200 Sonifier and particle size distributions were measured using a Malvern Mastersizer E/2000 laser-sizer. To quantify suspended particulate matter (SPM) concentrations, water samples (1–5 L, depending on sediment concentrations) were filtered through 0.45 μm Millipore mixed cellulose esters membrane filters or 0.7 μm Whatman GF/F filters. The filters were dried for 2 h at 60°C and weighed. Three deionized water blanks—using the same water volume and filter type as with the bulk samples—were processed identically per batch of samples to be used as controls. The organic content was estimated by loss on ignition (LOI) on the dried and weighed filters. Filters were ignited at 550°C for 2 h and subsequently weighed. Triplicate blanks were processed similarly for each batch of samples.

Bacterial production and cell counts

Measurements of bacterial production and abundance were made on bulk water and free-living (< 1.6 μm) fractions. Bacterial production was estimated from ^{3}H-thymidine incorporation rates (Riemann et al. 1982). Triplicate incubations with ^{3}H-thymidine and either bulk water or 1.6 μm-filtered water were set up in 100 mL glass bottles, with three additional sterile-filtered samples (0.2 μm) per set of bottles as blanks. ^{3}H-thymidine was added to the live triplicates to a final concentration of 10 nmol L^{-1}. Based on a different study, ^{3}H-thymidine incorporation rates increased rapidly with increasing substrate concentrations up to 10 nmol L^{-1}, but rates increased only incrementally above this concentration (Hollibaugh 1988). Blank samples were immediately fixed with 0.5 mL of 100% trichloroacetic acid (TCA), and all samples were incubated for 6–8 h at in situ temperature on a small plankton wheel to ensure that particles remained suspended. After incubation, live samples were fixed with 0.5 mL of 100% TCA. Live and blank samples were then filtered through 0.2 μm cellulose nitrate filters that were prewashed with MilliQ, using filtration manifolds that were prechilled at −20°C. Glass vials and filtration towers were rinsed five times with approximately 200 mL of 5% ice cold TCA. Filters were stored at −20°C in plastic vials and transferred back to the institutional laboratory, where 5 mL of scintillation cocktail was added and the samples were counted on a Perkin Elmer Liquid Scintillation Analyzer (Tri-Carb 2800TR). Results were converted to bacterial production by assuming production of 2.0×10^{18} cells per mole of ^{3}H thymidine fixed (Smith and Clement 1990).

Samples for bacterial cell counts were fixed in 0.5% glutaraldehyde and stored at 5°C. The cell numbers were quantified in both bulk water and free-living fractions (< 1.6 μm) by flow cytometry (BD FACSCanto II). Prior to analysis, bulk samples with particles were sonicated for 15 s three times to release the particle associated communities, and cells were stained with SYBR Green I (Molecular Probes, Eugene, Oregon, U.S.A.) at a final concentration of 10^{-4} of the commercial stock solution following the procedure of Marie et al. (1999). Samples containing high concentrations of inorganic particles were diluted 5–20 times in TRIS-EDTA buffer to eliminate interference during quantification.

Peptidase and glucosidase activity assays

Activities of five exo- (terminal cleaving) and endo-acting (mid-chain cleaving) peptidases were measured using low-molecular-weight substrate analogs labeled with 7-amido-4-methylcoumarin (MCA): Leucine-aminopeptidase (Leucine-MCA), AAF-chymotrypsin (Alanine–Alanine-Phenylalanine-MCA), AAPF-chymotrypsin (Alanine–Alanine-Proline-Phenylalanine-MCA), FSR-trypsin (Phenylalanine-Serine-Arginine-MCA), QAR-trypsin (Glutamine-Alanine-Arginine-MCA). Additionally, activities of two glucosidases were also measured using substrate analogs labeled with 4-methylumbelliferone (MUF): α-glucosidase (α-D-glucopyranoside-MUF), and β-glucosidase (β-D-glucopyranoside-MUF). Leucine aminopeptidase cleaves peptide bonds adjacent to leucine residues (Obayashi and Suzuki 2005)—as well as other amino acids through non-specific hydrolysis (Steen et al. 2015)—at the N-terminus. Chymotrypsins are endopeptidases that hydrolyze midchain peptide bonds next to a large hydrophobic amino acid, such as phenylalanine. Trypsins are also endopeptidases that cleave midchain peptide bonds adjacent to arginine. α-glucosidase cleaves bonds that release α-linked glucose, whereas β-glucosidase hydrolyzes bonds that free β-linked glucose (Barman 1969). These substrates were chosen to measure a range of exo-acting and endo-acting enzymes (Obayashi and Suzuki 2005; Steen and Arnosti 2013) that hydrolyze proteins and carbohydrates, which are typical constituents of OM (Benner 2002). However, as these

substrates do not reflect the structural complexity and diversity of natural organic compounds, we additionally used high-molecular-weight polysaccharide substrates to measure other potentially active hydrolytic enzymes (*see* "Polysaccharide hydrolase measurements" section).

All seven low-molecular-weight substrates were used to measure bulk water and particle-associated (≥ 1.6 μm) enzymatic activities. Note that all enzyme activities measured here are potential activities, since substrates added compete with naturally occurring substrates for enzyme active sites (Hoppe 1983). Enzyme activities were measured in triplicate in bulk water by adding 4 mL of the sample to replicate cuvettes. An incubation containing autoclaved water (with substrate added after the water had cooled to room temperature) served as the killed control. This procedure was used for each of the seven substrates; in addition, for each site and depth, there was one live blank (no substrate added) and one autoclave blank (no substrate, only autoclaved water), resulting in 30 parallel incubations per site/depth. Each cuvette containing either live or autoclaved water was amended with one substrate to a concentration of 100 μmol L^{-1}. This concentration has been used in enzymatic assays from other parts of the Arctic (Sala et al. 2010; Arnosti 2015; Balmonte et al. 2018), although substrate saturation curves with Svalbard fjord waters indicate that this concentration—while close to substrate saturating conditions—may underestimate V_{max} of several enzymes by factors of 1.5–2.8 (Steen and Arnosti 2013). The high cost of the trypsin and chymotrypsin substrates in any case limit the use of these substrates at higher concentrations.

To measure particle-associated enzyme activities, water samples were size-fractionated through a Whatman GF/A filter using gravity filtration to capture ≥ 1.6 μm particles. Gravity-filtered water volumes ranged from approximately 1.02 L in the particle-rich rivers, up to 5.86 L in the subsurface waters of GS. GF/A filters containing particulate matter were evenly divided using sterile razor blades into 1/12th pieces. Each piece was submerged in a cuvette containing 4 mL of cooled, autoclaved water from the same station/depth as the live samples. In addition, killed controls consisted of sterile GF/A filters cut into 1/12th pieces. One killed control and duplicate live filter incubations were used for each of the seven substrates, totaling 21 incubations per site/depth. Bulk water and particle-associated enzyme assays were incubated for up to 24 h and 16 h, respectively, and fluorescence was measured at specific intervals (excitation: 365 nm; emission: 440–470 nm) using a Turner Biosystems TBS-380 solid-state fluorimeter. Incubations were kept in the dark either at 0°C, 5°C, or 8°C, depending on in situ water temperature at the time of sampling.

Polysaccharide hydrolase measurements

Activities of polysaccharide hydrolyzing enzymes in bulk water and associated with particles (≥ 1.6 μm) were measured using six structurally distinct polysaccharides: pullulan [α(1,6)-linked maltotriose], laminarin [β(1,3-glucose)], xylan (xylose), fucoidan (sulfated fucose), arabinogalactan (arabinose and galactose), and chondroitin sulfate (sulfated *N*-acetylgalactoseamine and glucuronic acid) (Arnosti 2003; Teske et al. 2011). These substrates were chosen as they are produced by phytoplankton (Painter 1983) and terrestrial plants, as is the case for xylan (Opsahl and Benner 1999), Additionally, mono- and oligomers of these polysaccharides are detected in the marine organic matter pool (Benner 2002), as well as on the surface of the Greenland Ice Sheet (Stibal et al. 2010). Enzymes hydrolyzing these polysaccharides have been demonstrated to occur in marine bacteria (e.g., Alderkamp et al. 2007; Elifantz et al. 2008; Neumann et al. 2015).

Bulk water incubations were carried out following established procedures (Teske et al. 2011; Balmonte et al. 2018). Briefly, 15 mL of bulk water (in triplicate) and a single 15 mL sample of autoclaved water (as a killed control) were amended with a single substrate at a concentration of 3.5 μmol L^{-1} monomer equivalent. Due to its lower fluorescence, fucoidan was added to a final concentration of 5.0 μmol L^{-1} monomer equivalent. These concentrations were chosen to ensure sufficient fluorescent signal detection, and represent an addition of 21–30 μmol L^{-1} C. Note that adding higher concentrations of fluorescently labeled polysaccharides to samples would not change the hydrolysis rates measured, but could delay the timepoint at which hydrolysis is detected, since hydrolysis is determined as the change in molecular weight of the total added polysaccharide pool (Arnosti 2003). A live blank and an autoclave blank were included in each sample set, resulting in 26 incubations per site/depth. For particle-associated measurements, GF/A filters containing particulate matter—as described in "Peptidase and glucosidase activity assays" section—were also used. Each filter piece was submerged in 15 mL of cooled, ambient autoclaved water; the live filter incubations were done in duplicates. One sterile GF/A filter bit was used as a single killed control per substrate. In total, 21 particle-associated incubations were made for each site/depth.

Samples were incubated in the dark at near in situ temperature (0°C, 5°C, or 8°C), and subsampled at specific time intervals—t_0 (0 h, upon substrate addition), t_1 (120 h), t_2 (240 h), t_3 (360 h), and t_4 (600 h). Subsamples at each timepoint were filtered through 0.2 μm pore size surfactant-free cellulose acetate syringe filters, and the filtrate was collected and frozen at −20°C until processing in the lab. Samples were processed using gel permeation chromatography with fluorescence detection, and hydrolysis rates were calculated from changes in molecular weight of added substrates (Arnosti 2003). To focus on maximum community potential, we report the maximum rates throughout the incubation in the main text. Maximum rates come from different timepoints, and represent the greatest change in substrate molecular weight per unit time during our incubation time course. Data for all timepoints are in the Supporting Information Fig. S1A–F.

For all enzyme activity data, permutational analysis of variance (PERMANOVA) implemented on the R Package *vegan* (Oksanen et al. 2013) with the "adonis" function was used to partition the variations explained by sample type (bulk water vs. particles), differences in salinity, bacterial cell counts, and bacterial production. As the biotic variables did not significantly correlate with differences in enzyme activities, we only retained sample type and salinity in the models. Bray-Curtis dissimilarity index was used to calculate a dissimilarity matrix for the enzyme activity rates.

Bacterial community composition analyses

At all sites and depths, approximately 1 L of water was collected and filtered through a 0.2 μm Nucleopore membrane filter to capture bacteria for bulk water (nonsize-fractionated) bacterial community analyses. Filters with bacteria were stored at −80°C until subsequent DNA extraction and analyses. DNA was extracted from both the 0.2 μm Nucleopore membrane filters and the 1.6 μm GF/A filters (unused 1/12th pieces after particle-associated enzyme activity assays were set up). The Qiagen PowerSoil DNA Extraction kit was used following the manufacturer's protocol. DNA samples were sent to the UNC Core Microbiome Sequencing Facility to sequence 16S rRNA genes using Illumina MiSeq PE 2 × 250, targeting the V1-V2 hypervariable region with the bacterial primers 8F (5′- AGA GTT TGA TCC TGG CTC AG −3′) and 338R (5′- GCT GCC TCC CGT AGG AGT −3′). Sequence pairs were merged using fastq-join on QIIME (Caporaso et al. 2010). Merged reads were quality filtered, removing reads with 70% of the sequence below a phred score of 24; quality control was verified by FastQC. Operational taxonomic units (OTUs, 97% sequence similarity) were picked de novo using default parameters on QIIME. Chimeric sequences were identified and removed using ChimeraSlayer (Haas et al. 2011), and sequences that were not present in at least two samples were removed. Greengenes database was used to classify the remaining OTUs (DeSantis et al. 2006). OTUs detected in the sequencing blank were excluded from further analyses. Raw sequence files have been uploaded on the NCBI Sequence Read Archive with the accession numbers SRP140671.

The R package *phyloseq* (McMurdie and Holmes 2013) was used to rarefy the data set to 85,000 sequences per sample. Canonical analysis of principal coordinates (CAP) was conducted on the sequence data set with the Bray-Curtis dissimilarity index using *vegan* (Oksanen et al. 2013). Analyses of community dissimilarity (Bray-Curtis) on groupings of bacterial communities were conducted using the function "anosim" (analysis of similarity [ANOSIM]) in the package *vegan* with 999 permutations. The relationship between bacterial community dissimilarity and various environmental parameters was analyzed using PERMANOVA, as described above.

DOM composition analyses

Water samples were initially filtered through GF/F filters to remove larger particles and then processed largely following Dittmar et al. (2008), by acidifying prior to extraction on precleaned (12 mL methanol, MS-grade) PPL cartridges (Agilent Bond Elut PPL, 1 g resin, 6 mL volume). While DOM extraction efficiency was not measured in this study, a previous comparison using river and brackish vs. marine water samples from different regions indicated about 60% (river and brackish) vs. 43% (marine) extraction efficiencies (Dittmar et al. 2008). Cartridges were rinsed with 0.01 mol L^{-1} HCl, and the concentrated DOM was eluted using 12 mL methanol (MS-grade), and stored in muffled 20 mL glass vials. Samples were stored at −80°C until mass spectroscopic analyses.

To obtain a molecular fingerprint of the DOM pool, samples were analyzed on a 6530-LC-QTOF-MS (Agilent Technologies, Santa Clara, U.S.A.) using chromatographic and mass spectrometric settings, and feature extraction algorithms as previously described (Hasler-Sheetal et al. 2016) with slight modifications. Two milliliters of sample was dried in a speed-vac and reconstituted in 100 μL of 0.1% formic acid in a methanol:water mix before analysis on LC-QTOF-MS (Hasler-Sheetal et al. 2015). In a separate analysis, the relative concentrations of specific substrates—including glucose, arginine, proline, and leucine—were quantified to couple the rates of specific enzyme activities with relative concentrations of enzymatic hydrolysis products. Samples were derivatized, and glucose, arginine, proline, and leucine were measured in concentrated DOM against standards using a 7200 GC-QTOF-MS (Agilent Technologies, Santa Clara, U.S.A.) following a previously established method (Hasler-Sheetal et al. 2016). A complete DOM data set is not available because samples from Tyroler and Lerbugten Rivers were lost during transit.

The differences in DOM composition were analyzed using CAP based on Bray-Curtis dissimilarities of ranked and square root transformed data. The significance of dissimilarities between groups was evaluated using "anosim" in the R package *vegan*. The relationship between DOM composition and bacterial community (Bray-Curtis) dissimilarities was evaluated using Mantel test. A similar analysis, conducted on DOM composition dissimilarity calculated using Euclidean distances, yielded similar results. Partial Mantel test was used to test this relationship independent of salinity differences. All linear regressions, including those between specific DOM compounds and enzymatic activities, as well as between bacterial parameters and salinity, were performed using the "lm" function on R.

Results

Water mass and particle characteristics

Rivers in Tyrolerfjord-Young Sound contained freshwater with high SPM concentrations (Table 1), ranging from 234.4 to 552.3 mg L^{-1}, likely due to subglacial and terrestrial

Table 1. Physical, geochemical, and bacterial parameters measured in rivers. Standard deviations are shown where replicate measurements are available.

	Tyro-R	Ler-R	Zac-R
Depth (m)	1	1	1
Temperature (°C)	2.2	1.9	4.2
Salinity (PSU)	0	0	0
Turbidity (FTU)	NA	NA	NA
Oxygen (μmol L^{-1})	NA	NA	NA
SPM (mg L^{-1})	316.1	552.3	234.4
LOI (%)	4.8	2.5	6.3
Mean particle size (μm)	8.5	17.8	5.7
BP—bulk (μg C L^{-1} d^{-1})	0.33 ± 0.03	3.03 ± 0.42	3.28 ± 0.72
BP—PA (μg C L^{-1} d^{-1})	0.24	0.73	3.11
BP—FL (μg C L^{-1} d^{-1})	0.09 ± 0.01	2.29 ± 0.10	0.16 ± 0.06
BA—bulk (10^6 cells mL^{-1})	0.29 ± 0.02	0.15 ± 0.03	0.51 ± 0.09
BA—PA (10^6 cells mL^{-1})	0.19	0.08	0.24
BA—FL (10^6 cells mL^{-1})	0.10 ± 0.08	0.07 ± 0.03	0.27 ± 0.01

BA, bacterial abundance (cell counts); BP, bacterial production; FL, free-living; LOI, loss on ignition; NA, data not available; PA, particle-associated; SPM, suspended particular matter.

influence. River plumes contained a mixture of freshwater and marine waters (12.55–15.52 PSU), with SPM concentrations that gradually decreased along the river-fjord transition, reaching values of only 7.8–95.3 mg L^{-1}. Subsurface waters (20 m) at the river transition sites were largely marine in origin (31.33–31.52 PSU), and exhibited some of the lowest SPM values, in the range of 2.0–5.8 mg L^{-1} (Table 2). Within the fjord, surface waters were marine with comparatively little freshwater signature, as indicated by salinity (27.83–29.05 PSU); subsurface waters showed higher salinity values (29.48–31.23 PSU). SPM values in the fjord were low, in the range of 1.2–7.7 mg L^{-1} (Table 3). In rivers, LOI values—a proxy for OM content—were on average lower (2.5–6.3%; Table 1) compared to those within the fjord (Table 3). In the river plumes, LOI ranged from 9.2% to 10.1%, while those in subsurface waters of the river transition sites were higher (22.2–23.1%). LOI values in surface and subsurface waters within the fjord included the highest values measured, ranging from 12% to 40%. The smallest particles were found in Zac-R (5.7 μm), but mean particle size from Ler-R (17.8 μm) was comparable to those in the river transition sites (Table 3). In the fjord, particles were even larger, and ranged from 10.4 to 29.6 μm (Table 3).

Bacterial cell counts and production

Bulk bacterial cell counts were lowest on average in rivers ($0.15 \pm 0.03 \times 10^6$ to $0.51 \pm 0.09 \times 10^6$ cells mL^{-1}), and highest in the fjord ($3.0 \pm 0.69 \times 10^6$ to $3.5 \pm 0.09 \times 10^6$ cells mL^{-1}); this spatial trend was also observed for the free-living and particle-associated communities (Tables 1–3). A linear regression of bacterial cell counts against salinity confirmed positive and statistically significant relationships, the strongest of which was observed for the free-living fraction (Supporting Information Fig. S2C). For most stations and depths, particle-associated bacterial cell counts were greater than those for the free-living community. Bacterial production measurements were highly variable and showed no general trend between environments (Supporting Information Fig. S3A–C). However, lowest rates of bulk bacterial production were measured in Tyro-R (0.33 μg C L^{-1} d^{-1}; Table 1) and in the surface and subsurface waters of Tyro-T (0.46 μg C L^{-1} d^{-1} and 0.26 μg C L^{-1} d^{-1},

Table 2. Physical, geochemical, and bacterial parameters measured in river transition sites. Standard deviations are shown where replicate measurements are available.

	Tyro-T surface	Tyro-T subsurface	Ler-T surface	Ler-T subsurface	Zac-T surface	Zac-T subsurface
Depth (m)	2	20	2	20	2	20
Temperature (°C)	7.94	−0.27	6.22	0.29	0.2	0.1
Salinity (PSU)	12.55	31.52	15.52	31.33	22.3	29.9
Turbidity (FTU)	34.4	6.4	30.4	7.8	28.3	10.1
Oxygen (μmol L^{-1})	336.7	403.8	338.3	409.1	335.3	411.1
SPM (mg L^{-1})	7.8	2	71.5	5.8	95.3	4.4
LOI (%)	9.2	22.2	NA	NA	10.1	23.1
Mean particle size (μm)	9.3	12.1	10.5	NA	15	16.7
BP—bulk (μg C L^{-1} d^{-1})	0.46 ± 0.10	0.26 ± 0.13	1.99 ± 1.03	2.03 ± 0.82	1.09 ± 0.44	1.20 ± 0.09
BP—PA (μg C L^{-1} d^{-1})	0.06	0	1.44	0.62	0.76	0.96
BP—FL (μg C L^{-1} d^{-1})	0.40 ± 0.10	0.27 ± 0.19	0.55 ± 0.23	1.41 ± 0.30	0.32 ± 0.08	0.23 ± 0.23
BA—bulk (10^6 cells mL^{-1})	1.10 ± 0.01	0.32 ± 0.07	0.57 ± 0.07	3.90 ± 0.11	2.90 ± 0.58	2.20 ± 0.19
BA—PA (10^6 cells mL^{-1})	0.41	0	0.14	2.50	2.17	1.43
BA—FL (10^6 cells mL^{-1})	0.69 ± 0.05	0.76 ± 0.16	0.43 ± 0.06	1.40 ± 0.41	0.73 ± 0.06	0.77 ± 0.06

BA, bacterial abundance (cell counts); BP, bacterial production; FL, free-living; LOI, loss on ignition; NA, data not available; PA, particle-associated; SPM, suspended particular matter.

Table 3. Physical, geochemical, and bacterial parameters measured in the fjord. Standard deviations are shown where replicate measurements are available.

	YS-1 surface	YS-1 subsurface	YS-2 surface	YS-2 subsurface	GS surface	GS subsurface
Depth (m)	5	20	5	20	5	20
Temperature (°C)	2.74	0.15	1.14	−0.44	−1.42	−1.5
Salinity (PSU)	27.83	31.13	29.26	31.23	29.05	29.48
Turbidity (FTU)	9.3	1.9	4.1	2.2	8.7	3.3
Oxygen (μmol L^{-1})	361.8	392.6	370.2	381.6	372.7	381.0
SPM (mg L^{-1})	NA	NA	1.2	NA	7.7	2.4
LOI (%)	38	21.3	NA	NA	12	40
Mean particle size (μm)	29.6	10.4	NA	NA	NA	NA
BP—bulk (μg C L^{-1} d^{-1})	2.36 ± 0.86	1.16 ± 0.17	4.39 ± 0.48	3.45 ± 1.24	NA	NA
BP—PA (μg C L^{-1} d^{-1})	0.57	0.53	2.16	1.01	NA	NA
BP—FL (μg C L^{-1} d^{-1})	1.80 ± 0.26	0.62 ± 0.05	2.24 ± 1.01	2.44 ± 0.87	NA	NA
BA—bulk (10^6 cells mL^{-1})	NA	NA	3.50 ± 0.09	3.00 ± 0.69	NA	NA
BA—PA (10^6 cells mL^{-1})	NA	NA	2.40	1.90	NA	NA
BA—FL (10^6 cells mL^{-1})	NA	NA	1.10 ± 0.34	1.10 ± 0.19	NA	NA

BA, bacterial abundance (cell counts); BP, bacterial production; FL, free-living; LOI, loss on ignition; NA, data not available; PA, particle-associated; SPM, suspended particular matter.

respectively; Table 2). Highest rates of bulk bacterial production were observed at Ler-R and Zac-R (Table 1). Particle-associated bacterial production was lowest at both depths in Tyro-T (Table 2), and highest at Zac-R (Table 1).

Peptidase and glucosidase activities

The activity of a range of enzymes that cleave amino acid or glucose residues from organic compounds exhibited contrasting patterns from rivers to the fjord. The sums of peptidase and glucosidase activities (summed activities) in bulk waters were lower in rivers than in river transition sites and in the fjord (Supporting Information Fig. S4A). Among the rivers, highest summed activity was measured at Zac-R, while summed activities at Tyro-R and Ler-R were comparable, although the relative contributions of enzyme activities differed. In river transition sites, highest summed activities were measured at Zac-T, while the lowest were found in Ler-T. In fjord sites, the highest summed activities were measured at YS-1—at the confluence of Zackenberg and Lerbugten River outflow. Summed peptidase and glucosidase activities in bulk waters showed a moderate, but statistically significant positive correlation with cell counts (R^2 = 0.42, p = 0.018) (Supporting Information Fig. S5A).

Bulk water peptidase and glucosidase activities showed contrasting patterns across the salinity gradient. Leucine aminopeptidase activities were consistently detected at all sites, but were highest in the fjord (Fig. 2A). For the two chymotrypsin substrates, AAPF-chymotrypsin showed higher activities than AAF-chymotrypsin; AAF-chymotrypsin activities were not measurable at every site, and were lowest in rivers and higher at all sites in the fjord. The activities of both types of trypsin enzymes generally increased along the salinity gradient, but QAR-Trypsin had higher activities overall than FSR-trypsin. In contrast to peptidase trends, glucosidase activities tended to decrease with increasing salinity (Fig. 2A). Overall, salinity differences accounted for 30% of the variations among bulk water peptidase and glucosidase activities (PERMANOVA, R^2 = 0.30, p = 0.008).

Particle-associated peptidase and glucosidase activities exhibited some patterns along the salinity gradient that were similar to those in bulk waters, but diverged strongly in other cases. For example, summed particle-associated peptidase and glucosidase activities were higher in the fjord than in the rivers (Supporting Information Fig. S4B), a pattern that was likely driven in part by higher cell counts in the fjord (R^2 = 0.61, p = 0.003) (Supporting Information Fig. S5B). This pattern was also observed in bulk water (Supporting Information Figs. S4A, S5A); however, in the free-living fraction, the relationship between cell counts and summed peptidase and glucosidase activities was not statistically significant (Supporting Information Fig. S5C). Some substrate-specific trends were also similar in bulk water and on particles, as evident by leucine aminopeptidase activities (Fig. 2B). In contrast, particle-associated AAPF-chymotrypsin activities had a notably different pattern across the salinity gradient compared to that of bulk water. Furthermore, particle-associated rates (normalized to the volume of water filtered to obtain the particles) were generally lower than rates measured in bulk seawater (Fig. 2B). Considering only the particle-associated fraction, salinity explained 38% of the differences in peptidase and glucosidase activities across all sites (PERMANOVA, R^2 = 0.38, p = 0.002).

Polysaccharide hydrolase activities

In bulk waters, the spectrum and activities of polysaccharide hydrolases—which initiate the enzymatic cleavage of

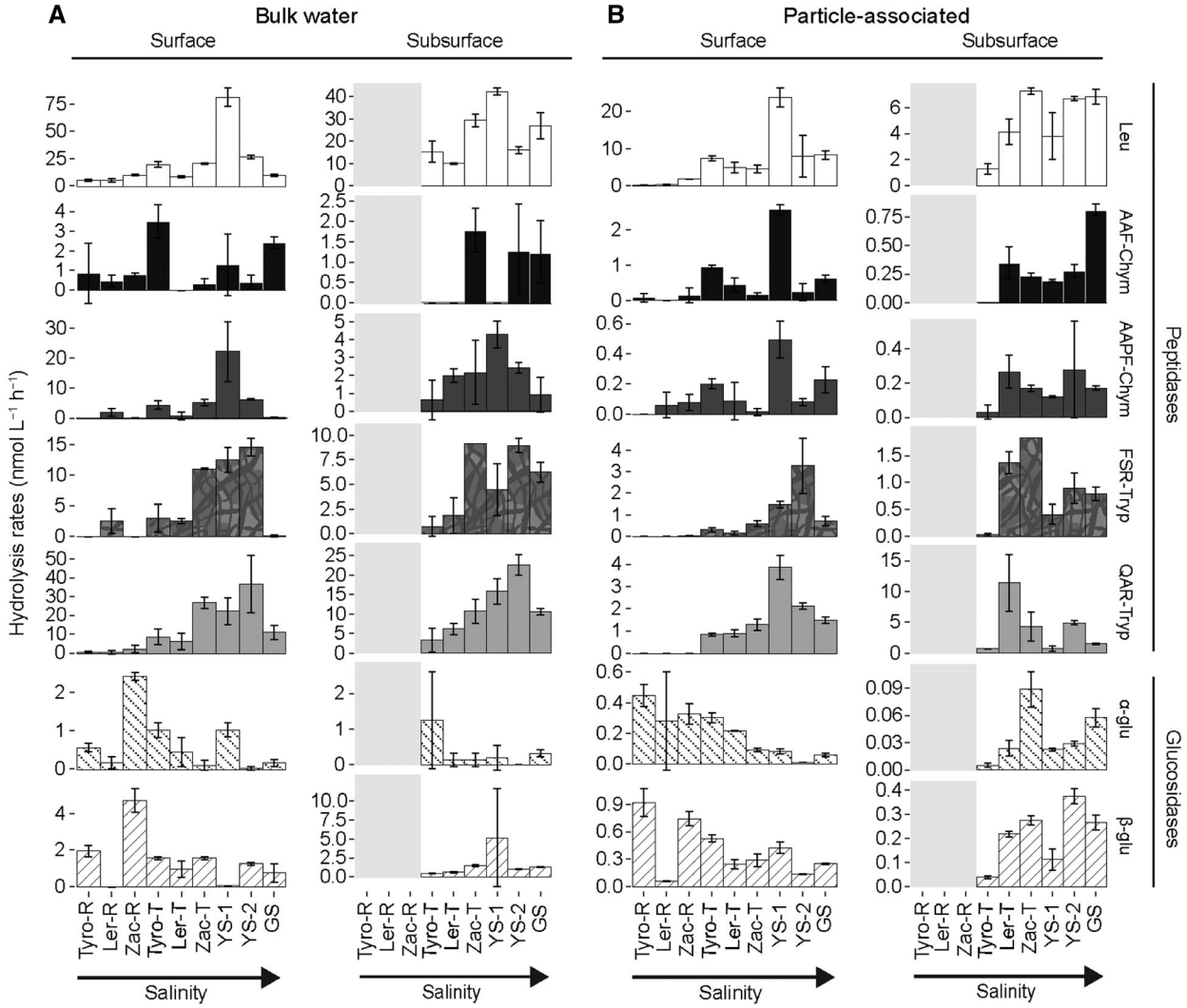

Fig. 2. Bulk water (**A**) and particle-associated (**B**) peptidase and glucosidase activities shown by substrate. The light gray shading in the panels indicates that no subsurface measurements were taken in the rivers. Within each plot, stations are arranged by salinity (increasing to the right), and from the inner to the outer part of the fjord. Note the differences in scale across all plots. Reported rates are averaged from triplicate (bulk water) or duplicate (particle-associated) incubations, and measured 12 h after the start of incubation. α-glu, α-glucopyranoside; β-glu, β-glucopyranoside; AAF-Chym, alanine-alanine-phenylalanine-chymotrypsin; AAPF-Chym,-alanine-alanine-proline-phenylalanine-chymotrypsin; FSR-Tryp, phenylalanine-serine-arginine-trypsin; Leu, leucine; QAR-Tryp, glutamine-alanine-arginine-trypsin.

diverse, naturally occurring polysaccharides found in aquatic OM pools—showed considerable contrasts between the rivers compared to river transition and fjord sites (Fig. 3A, Supporting Information Fig. S6A). Salinity differences accounted for 37% of the variation in polysaccharide hydrolysis patterns (PERMANOVA, $R^2 = 0.37$, $p = 0.001$). In rivers, only laminarin and xylan were consistently hydrolyzed, although very low rates of pullulan and chondroitin hydrolysis were also measured in Zac-R (Fig. 3A). In surface and subsurface waters of river transition sites, only laminarin was hydrolyzed at all sites; xylan, chondroitin, and pullulan hydrolysis were also measured in most of the river plume waters. In subsurface bulk waters of river transition sites and bulk waters at both depths in fjord sites, laminarin, chondroitin, and xylan were consistently hydrolyzed. Pullulan was hydrolyzed at most of these sites, while fucoidan was only measurably hydrolyzed at YS-1. Arabinogalactan was not detectably hydrolyzed in bulk waters. Furthermore, the rate at which xylan and chondroitin were hydrolyzed exhibited robust trends across the salinity gradient. Highest rates of xylan hydrolysis were measured in the rivers (Fig. 3A). In contrast, rates of chondroitin hydrolysis peaked in the fjord, but hydrolysis was very low or undetectable in rivers (Fig. 3A).

A wider spectrum of polysaccharides was hydrolyzed on particles compared to bulk waters (Fig. 3B, Supporting Information Fig. S6B). Laminarin, xylan, chondroitin, and pullulan were consistently hydrolyzed on particles in rivers (Fig. 3B). In river transition sites, laminarin, xylan, and pullulan hydrolysis were consistently measured. Chondroitin was hydrolyzed on particles from all river transition sites, with the exception of

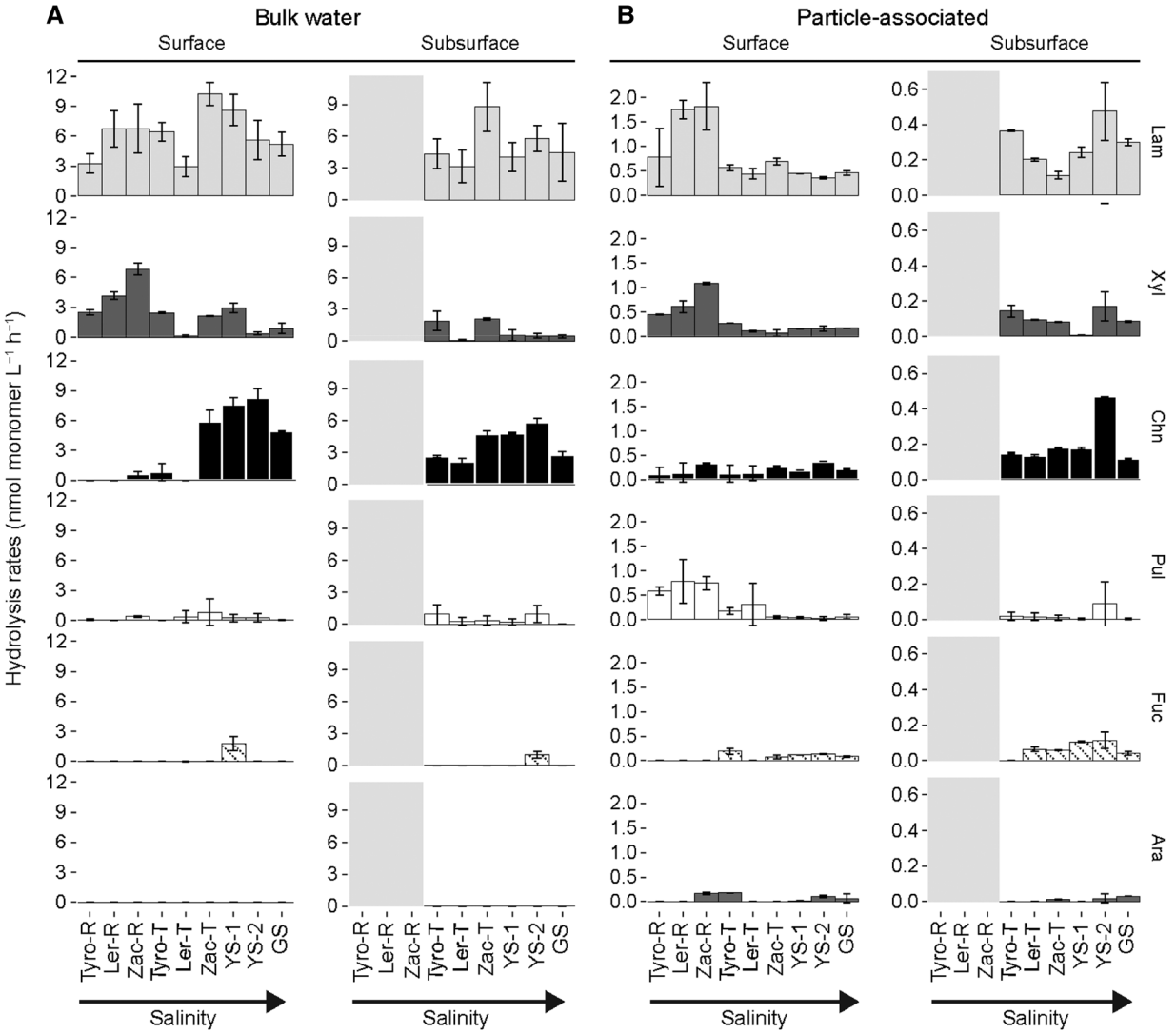

Fig. 3. Bulk water (**A**) and particle-associated (**B**) polysaccharide hydrolase activities shown by substrate. The light gray shading in the panels indicates that no subsurface measurements were taken in the rivers. Within each plot, stations are arranged by salinity (increasing to the right), and from the inner to the outer part of the fjord. Note the scale differences. Reported rates are averaged from triplicate (bulk water) or duplicate (particle-associated) incubations, and taken at different timepoints throughout the incubation. See Supporting Information Fig. S1A–F for all rates. Ara, arabinogalactan; Chn, chondroitin sulfate; Fuc, fucoidan; Lam, laminarin; Pul, pullulan; Xyl, xylan.

the surface water at Ler-T. Particle-associated fucoidan hydrolysis was also detected in most river transition sites; the exceptions were on particles from Ler-T surface water and Tyro-T subsurface water. Moreover, in river transition sites, arabinogalactan hydrolysis was only detected on particles from Tyro-T surface water and Zac-T subsurface water. Particle-associated polysaccharide hydrolysis rates at river transition sites were generally lower in subsurface waters compared to surface waters. In the fjord, laminarin, chondroitin, and fucoidan were consistently hydrolyzed on particles. Particle-associated xylan and arabinogalactan hydrolysis was detected at almost all fjord sites, with the exception of YS-1 subsurface waters. Pullulan hydrolysis was also detected on particles from almost all of the fjord sites, except at YS-1 and GS subsurface waters. Across all sites, the highest particle-associated summed rates were detected in rivers (Supporting Information Fig. S6B). Outside of the rivers, summed hydrolysis rates were generally higher in surface compared to subsurface waters. Salinity differences accounted for a greater portion (38% vs. 59%) of the variation in particle-associated polysaccharide hydrolase activities (PERMANOVA, $R^2 = 0.59$, $p = 0.001$), compared to particle-associated trends for peptidase and glucosidase activities.

Spatial patterns in bacterial community composition

Bacterial communities grouped into three clusters with significant compositional differences (ANOSIM, $R = 0.997$, $p = 0.001$; Supporting Information Table S1), and which correlated significantly with salinity (PERMANOVA, $R^2 = 0.39$,

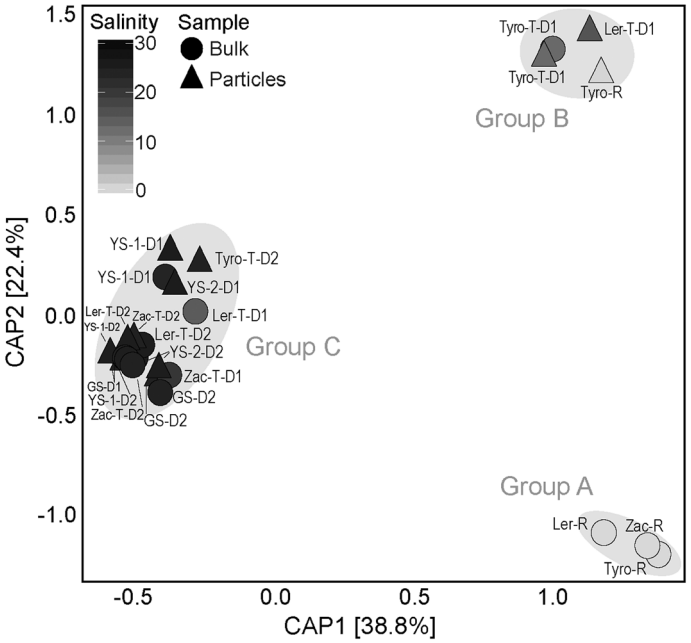

Fig. 4. Canonical analysis of principal coordinates of bacterial community composition using Bray-Curtis dissimilarity index. OTU cutoff was set at 97% sequence similarity, and was picked using de novo methods. The groupings are significantly different based on ANOSIM. "D1" and "D2" denote surface and subsurface waters, respectively.

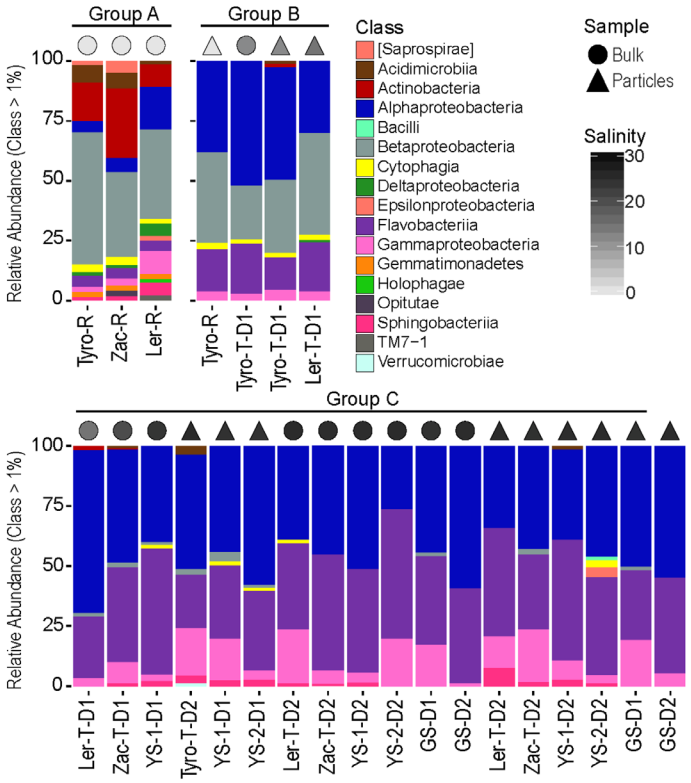

Fig. 5. Class-level taxonomic designation of bacterial communities, arranged from left to right in order of increasing salinity, and from the head to the mouth of the fjord. Only bacterial classes with relative proportions of ≥ 1% were visualized to deconvolute the plot. The groups and legends for the symbols above the bar graph are the same as those in Fig. 4. Square brackets around *Saprospirae* indicate the recommended taxonomic nomenclature based on genome trees in the Greengenes database. "D1" and "D2" denote surface and subsurface waters, respectively.

p = 0.001) (Fig. 4). Group A included the riverine bulk water communities, with members from a greater diversity of bacterial classes compared to communities in other clusters (Fig. 5). Some of these communities, however, showed surprisingly lower OTU-level diversity (species richness) compared to river-transition and fjord communities (Supporting Information Fig. S7), for which a narrower range of bacterial classes was detected (Fig. 5). Additionally, this freshwater cluster is characterized by low to moderate relative proportions—but high diversity—of *Alphaproteobacteria*. Moderate to large relative abundances of the class *Actinobacteria*, and large contributions of *Betaproteobacteria* also characterized the freshwater group (Fig. 5). Group B contained the Tyro-R particle-associated sample and most of the river transition samples. This group exhibited large relative proportions of *Betaproteobacteria* and *Actinobacteria*, similar to Group A; however, Group B contained greater proportions of *Flavobacteria* and *Alphaproteobacteria*, and lower diversity in bacterial classes. Group C included communities from fjord sites and two river transition sites (surface bulk community at Ler-T and Zac-T). Bacterial communities in this group were characterized by large relative contributions of *Flavobacteria, Alphaproteobacteria*, and moderate proportions of *Gammaproteobacteria*, as well as some of the highest observed OTUs in the data set (Supporting Information Fig. S7).

The difference between the particle-associated vs. bulk bacterial community was greater at Tyro-R compared to those in the river transition sites and in the fjord (Fig. 4); this comparison was only possible at Tyro-R due to low DNA extraction efficiency for other river particle samples. Furthermore, the Tyro-R particle-associated bacterial community exhibited high compositional similarity with the surface water of the river transition sites, and the bulk surface-water community at Tyro-T (Fig. 5). The observed differences were driven by changes in the relative proportions of specific members of *Alphaproteobacteria* and *Betaproteobacteria* (Fig. 5). Within *Alphaproteobacteria*, members of the family *Rhodobacteraceae* were detected in minimal to moderate relative proportions in bulk river communities—at about 4–20% of *Alphaproteobacteria*—but dominated the particle-associated alphaproteobacterial community at Tyro-R and river plumes; a similar trend was observed with members of the family *Alcaligenaceae* of the class *Betaproteobacteria*. In contrast, particle-associated communities in Group C were not significantly different compared to the bulk bacterial communities in the same waters (ANOSIM, R = 0.042, p = 0.275; Supporting Information Table S1).

DOM composition

A total of 15,439 DOM entities were detected using LC-QTOF-MS in the entire DOM data set, and were used as the molecular fingerprint of the DOM pool. CAP ordination

revealed three main pools of DOM that were statistically different from each other (ANOSIM, R = 0.629, p = 001): river water, river plume and marine mixture, and purely marine (Fig. 6). Thus, variations in the relative proportions of DOM components (Bray-Curtis dissimilarity) were correlated with salinity. Excluding samples from Zac-R—the only freshwater site where samples were available—three clusters formed: mid fjord, outer fjord, and coastal (Supporting Information Fig. S8); however, these groupings were not significantly different from each other (ANOSIM, R = 0.108, p = 0.224). Additionally, specific compounds (leucine, proline, arginine, and glucose) from the DOM pool, quantified against standards using GC-QTOF-MS, exhibited variable relative concentrations along the salinity gradient. Glucose was highest in Zac-R, whereas proline, arginine, and leucine were highest in the fjord (Supporting Information Fig. S10).

DOM, bacterial community, and enzymatic activity relationships

We analyzed correlations between bacterial community composition, enzymatic activities, and DOM composition across the salinity gradient. For the first analysis, only samples containing data for bacterial community composition and DOM composition were included (n = 11). Dissimilarities (Bray-Curtis) in the composition of bacterial community and DOM were significantly correlated (Mantel, r = 0.751, p = 0.004). Salinity differences also correlated with DOM composition (Mantel, r = 0.771, p = 0.01), similar to trends with bacterial community composition. Removing salinity differences from this relationship indicated spatial autocorrelation between bacterial community composition and DOM composition (partial Mantel test, r = 0.387, p = 0.126).

We further evaluated the relationship between activities of specific enzymes and relative concentrations of their putative hydrolysis products across the system. These analyses showed variability in the strength of the correlation between enzyme activities and relative proportions of hydrolysis products. For example, leucine aminopeptidase activities and relative concentrations of leucine were not correlated (Fig. 7A). In contrast, the relationship between the combined activities measured using the two trypsin-associated substrate proxies (QAR- and FSR-trypsin) with the relative concentrations of arginine—as well as the relationship between α- and β-glucosidase activities with glucose—were statistically significant (Fig. 7B,C). Because the relative concentrations of phenylalanine—the amino acid produced by the activity of AAPF-chymotrypsin—were unavailable, we correlated AAPF-chymotrypsin activities with relative proportions of proline, the amino acid to which phenylalanine is attached in our substrate analog; this analysis also showed a statistically significant positive relationship (Fig. 7D). A separate analysis with these data, excluding points that seemed to drive the significant positive relationship, showed similar results (Supporting Information Fig. S9A–C). Thus, with the exception of leucine, the relative concentrations of specific compounds (Supporting Information Fig. S10) followed the salinity-related trends exhibited by the peptidase and glucosidase activities.

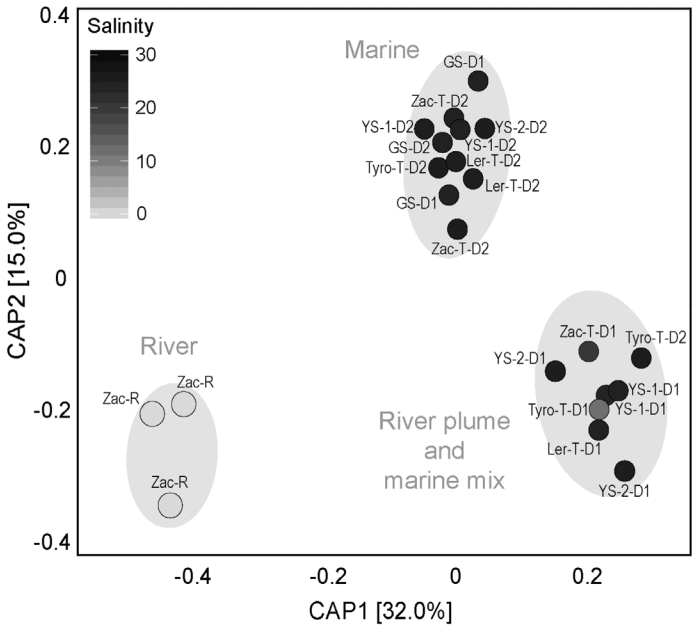

Fig. 6. Constrained analysis of principal coordinates of DOM composition using Bray-Curtis based dissimilarity index. Data were square root transformed. The groupings are significantly different based on ANOSIM. "D1" and "D2" denote surface and subsurface waters, respectively.

Discussion

Freshwater vs. marine microbial enzymatic capabilities

In a high latitude fjord, we show contrasting activities of hydrolytic enzymes (e.g., glucosidases, peptidases, and polysaccharide hydrolases) (Figs. 2–3) in river vs. fjord waters. These patterns illustrate distinct OM degrading capabilities of freshwater and marine microbial communities, indicating varied specialization to access and use different constituents of the OM pool. Functional differences parallel contrasting microbial community structure and DOM pools that reflect variations in salinity; the interactions between these three parameters are conceptualized in Fig. 8. Our use of a wide range of structurally diverse substrates—to measure the rates at which different microbial communities enzymatically hydrolyze widely occurring proteinaceous and carbohydrate constituents of natural OM pools (Benner 2002)—provided a broader range of comparisons for functional differences, expanding beyond the activities of commonly measured enzymes (e.g., leucine aminopeptidase and β-glucosidase). Compared to their counterparts in transition zones and marine waters, freshwater microbial communities exhibited, on average, twofold higher glucosidase and nearly fivefold greater xylanase activities (Figs. 2–3), based on measurements from bulk (nonsize-fractionated) waters. That highest glucosidase and xylanase activities measured in rivers is especially notable in light of low bacterial cell counts measured in these

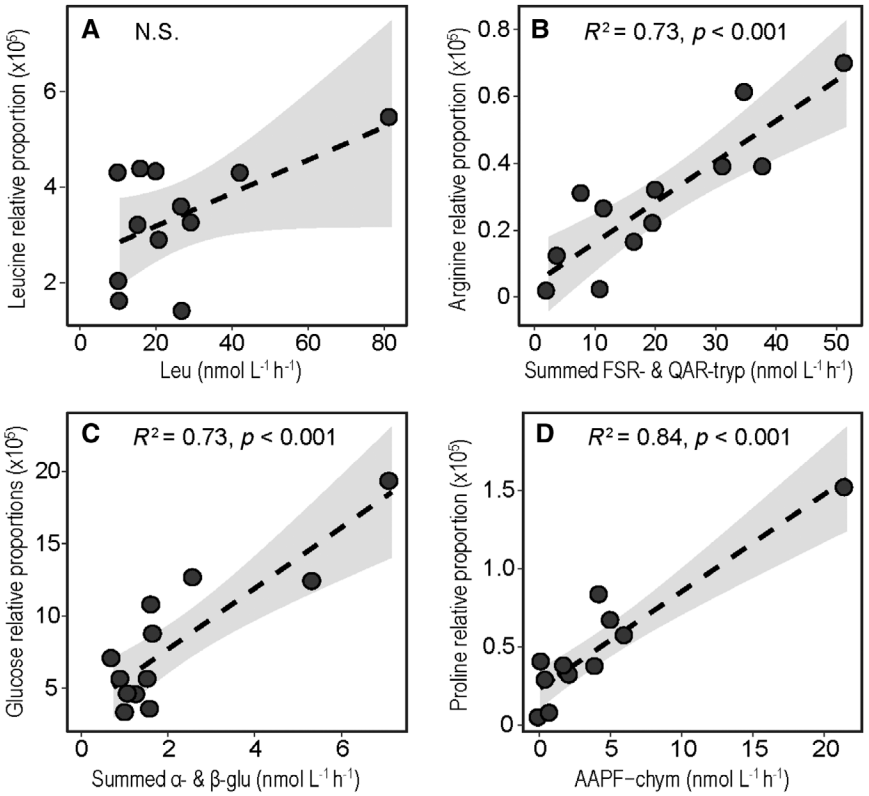

Fig. 7. Relationship between specific enzyme activities and the relative proportions of their putative hydrolysis products in DOM pools. The analysis included: (**A**) leucine aminopeptidase vs. leucine; (**B**) combined QAR- and FSR-trypsin vs. arginine; (**C**) combined α- and β-glucosidase vs. glucose; and (**D**) AAPF-chymotrypsin vs. proline. The gray band corresponds to the 95% confidence interval for predictions from the linear model. N.S. indicates a nonstatistically significant relationship.

waters (Tables 1–3). In contrast, bulk microbial communities in the fjord exhibited greater activities than those in rivers for all measured peptidase activities—from a 1.5-fold (AAF-chymotrypsin) up to a 15-fold difference in rates (QAR-trypsin) (Fig. 2; Supporting Information Fig. S5A). Chondroitin sulfatase activities were also much higher in the fjord, on average up to 30-fold, compared to those in the Zac-R, the only river where chondroitin was hydrolyzed (Fig. 3).

Contrasting freshwater and marine microbial enzymatic capabilities have also been observed in temperate and boreal waters. Several studies documenting high leucine aminopeptidase activities among marine microbes (Murrell et al. 1999; Cunha et al. 2000) have hypothesized these patterns to be due to (1) a greater diversity among marine bacterial taxa, or (2) evolutionary adaptations that enable these assemblages to produce a more effective set of enzymes to hydrolyze proteinaceous compounds (Stepanauskas et al. 1999). Higher diversity in Zac-R compared to sites within the fjord (Supporting Information Fig. S7) is inconsistent with the first hypothesis. However, the wide range of highly active (exo- and endo-acting) peptidases among marine microbial communities in our study (Fig. 2)—many of which have not been previously used to compare freshwater and marine microbial functionality—is in accordance with the second hypothesis. These patterns suggest that, compared to freshwater systems, coastal marine waters are sites of highly active protein degradation (Murrell et al. 1999); rapid remineralization of proteinaceous compounds has also been inferred following a phytoplankton bloom in two Svalbard fjords (Osterholz et al. 2014). In contrast, high β-glucosidase activities among freshwater microbial communities (Cunha et al. 2000) have been interpreted to suggest that these taxa specialize in carbohydrate-rich compound degradation (Murrell et al. 1999). However, polysaccharide hydrolase activities offer a much more nuanced view. Freshwater and marine microbes are attuned to hydrolyzing distinct types of polysaccharides, illustrated most robustly by differences in xylanase and chondroitin sulfatase activities (Figs. 3, 8; Supporting Information Fig. S6), used to access likely terrestrially derived polysaccharides and sulfated polysaccharides, respectively.

Differences in individual enzymatic activities and changes in enzymatic spectra do not scale with bacterial abundance and temperature across the freshwater–marine continuum, indicating that other biotic and abiotic parameters likely influence these profiles. For example, the effect of pH and salinity-driven conformational changes in DOM structure—as well as

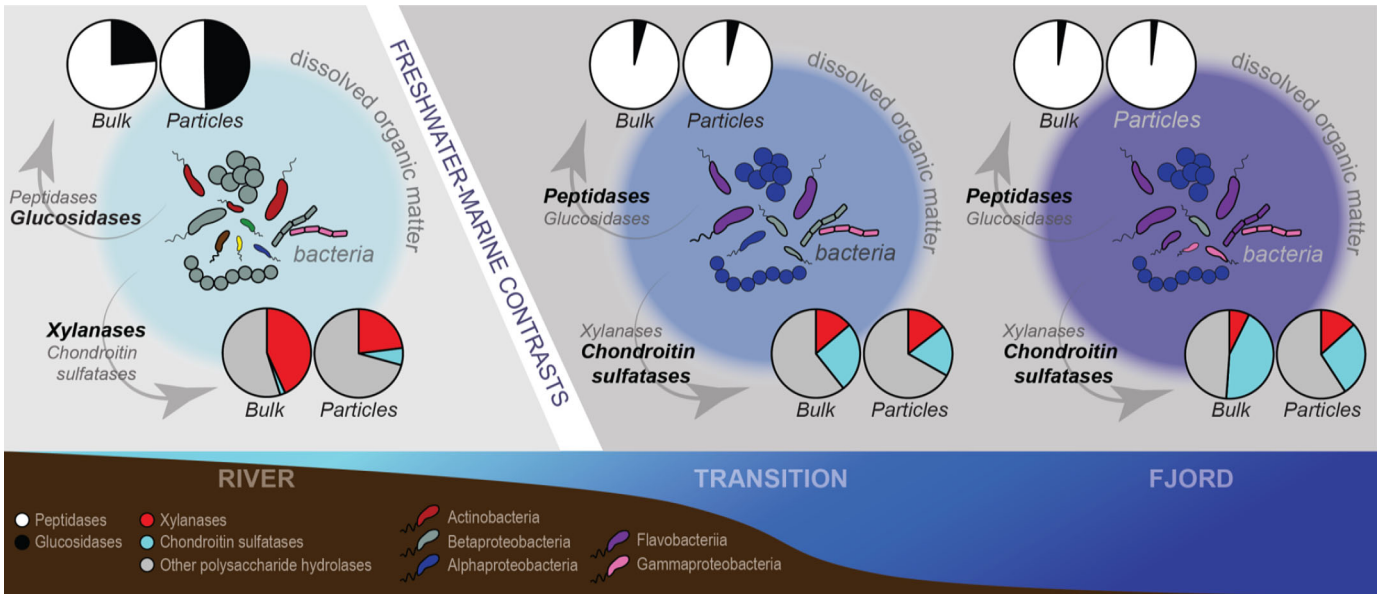

Fig. 8. Schematic diagram of freshwater and marine contrasts in bacterial community composition, enzymatic capabilities, and DOM pools. Enzymes in bold indicate a greater relative importance either in freshwater or marine water. Pie charts depict relative contributions of glucosidases and peptidases (top row) and polysaccharide hydrolases (bottom row) in bulk waters (left) and on particles (right) for each system (rivers, transition, fjord). DOM pools are colored according to salinity of water mass of origin. Bacterial communities are colored according to class-level taxonomic classification, as shown in Fig. 5, and depict higher class-level diversity in rivers.

differences in cation concentrations that are necessary for some enzyme activities (e.g., Mg^{2+} for aminopeptidase activity) or to prevent humus-enzyme complexes (Wetzel 1991)—may play a role in these observed patterns of enzyme activities and DOM bioavailability (Stepanauskas et al. 1999). As we do not address these parameters, we instead focus on mounting evidence for the links between enzymatic capabilities, contrasting community structure—including presumed differences in metabolic potential—and DOM supply across salinity gradients (Fig. 8).

Parallel patterns of enzyme activities and bacterial community composition

Potential coupling of microbial taxonomy and function suggests that differing enzymatic capabilities of freshwater vs. marine microbial communities can at least be partially attributed to variations in community composition (Figs. 4–5). Glacial meltwaters contain microbial taxa of freshwater (Stibal et al. 2012; Cameron et al. 2015) and terrestrial origins (Dubnick et al. 2017; Paulsen et al. 2017), and are similarly detected among riverine bacterial communities (Fig. 5). Riverine microbial taxa are unique from those at river transition sites (Figs. 4, 8), in which bulk bacterial communities are composed of typically marine members (Fig. 5), characterized by moderate to large proportions of *Alphaproteobacteria* (ca. 50–70%), and *Flavobacteria* (ca. 20–40%). Robust changes in community composition from rivers to river transition sites parallel a shift in the spectrum and rates of glucosidases, peptidase, and polysaccharide hydrolase activities (Figs. 2–3; Supporting Information Figs. S4, S6). Bacterial community composition in the middle and outer reaches of the fjord do not show large deviations from those in transition zones; similar proportions of *Alphaproteobacteria* and *Flavobacteria*—but occasionally larger contributions of *Gammaproteobacteria*, up to about 25% (Fig. 5)—are consistent with the composition of marine microbial communities in high latitudes (Gutiérrez et al. 2015; Balmonte et al. 2018). Thus, the influence of glacial meltwater on microbial communities in the fjord diminishes with distance from the rivers, as within-fjord microbial communities increasingly become structured by Greenland Sea coastal water inflow (Paulsen et al. 2017). As a result, strong freshwater–marine distinctions in community composition and enzymatic activity patterns are largely observed at river-to-fjord transition sites (Figs. 5, 8).

Differing enzymatic patterns between compositionally distinct freshwater and marine microbial assemblages are consistent with genomic suggestions that these microbial taxa possess distinct metabolic potentials for carbon processing (Ghai et al. 2011; Eiler et al. 2014). Specifically, genomic content of freshwater microbial communities includes high relative abundance of genes encoding glycoside hydrolases and xylose transporters compared to marine microbial metagenomes (Eiler et al. 2014), and may be the basis for the high glucosidase and xylanase activities in rivers (Figs. 2–3). In addition, greater relative abundance of genes for amino acid transporters detected in marine—compared to freshwater—microbial metagenomes (Eiler et al. 2014) may reflect microbial need for efficient uptake machinery for peptidase hydrolysis byproducts, such as those from highly

active leucine aminopeptidases, chymotrypsins, and trypsins within the fjord (Fig. 2).

Links between enzymatic activities and DOM composition

While genetic potentials may be rooted in microbial taxonomy, external DOM supply may exert a more immediate control of microbial enzymatic activities. In this study, DOM composition in rivers, river plume water, and within Tyrolerfjord-Young Sound exhibit differences that are strongly correlated with salinity, indicative of differences in water mass origins (Fig. 6; Supporting Information Fig. S8). The positive relationship between dissimilarities in DOM composition and bacterial community composition (Mantel $r = 0.751$, $p = 0.004$) in freshwater and marine sites implies that compositionally distinct communities interact with different DOM pools. Moreover, the positive relationship between several enzymatic activities and the relative concentrations of their putative hydrolysis products (Fig. 7) underscores the close association between the DOM pool and microbial heterotrophy, and links microbial enzymatic hydrolysis to outputs of their activities. Thus, while microbial composition and metabolic potential parallel substrate utilization patterns, differences in the rates and spectrum of peptide, glucose, and polysaccharide hydrolysis by freshwater vs. marine microbial taxa (Figs. 2–3) may reflect their response to varying OM pools in rivers and fjords. However, disentangling the relative influence of the composition of bacterial communities vs. the OM pool in shaping heterotrophic capabilities may be difficult. Evidence from boreal lakes and rivers suggests that microbial heterotrophic functionality is more tightly correlated with OM quality, whereas community structure covaries strongly with other physicochemical factors (Ruiz-González et al. 2015). Thus, salinity may more directly influence bacterial community composition and genetic potentials, but the extent to which hydrolytic enzymes are active could more closely reflect OM quality and quantity differences across the salinity gradient (Fig. 8).

Particle-associated contribution to enzymatic activities and community structure

Enzymatic activities measured on particles exhibited patterns consistent with as well as divergent from bulk water trends across the salinity gradient. Consistent with bulk water patterns, particle-associated glucosidase activities on a per volume basis were higher in freshwater vs. marine water, although to a much greater extent—up to eightfold higher for α-glucosidase and twofold greater for β-glucosidase (Fig. 2). Also in accordance with bulk water trends, particle-associated peptidase activities were more frequently detectable and higher in river transition sites and within the fjord than in rivers. These rate differences ranged from fivefold higher AAPF-chymotrypsin activities in marine particles, to undetectable FSR-trypsin and QAR-trypsin activities within river particles (Fig. 2). Moreover, a broader range of polysaccharide substrates were hydrolyzed on particles compared to the bulk water, regardless of location, as well as particle source and characteristics (Fig. 3; Supporting Information Fig. S6B); these patterns are especially evident for arabinogalactan and fucoidan hydrolysis, which were more frequently measured on particles than in bulk water. This particle-associated vs. bulk polysaccharide hydrolase difference in spectrum has been observed at various sites and depths in the central Arctic (Balmonte et al. 2018) and in the North Atlantic (D'Ambrosio et al. 2014). Moreover, carbohydrate content of particulate matter in fjords may shape particle-associated bacterial community structure, selecting for taxa that are likely capable of biopolymer degradation (Jain et al. 2019). Thus, particle-associated microbial taxa, compared to their free-living counterparts, may be equipped with a broader spectrum of hydrolytic enzymes that can hydrolyze high-molecular-weight components of particles, and likely contribute to the degradation and utilization of specific compounds transported from glacial catchments to the fjord.

As with bulk water trends, distinct particle-associated enzymatic activities may largely be due differences in bacterial community composition. For example, riverine particles host a bacterial assemblage distinct from that observed in bulk river waters, and this particle-associated community persists into river transition sites (Figs. 4–5). However, at the river transition sites, bulk community composition resembles that of high-salinity fjord sites, with the exception of surface-water Tyro-T, which also bears high similarity to the particle-associated community and retains a robust (ca. 25%) freshwater *Betaproteobacteria* signature (Tyro-T-D1; Figs. 4–5). This observation is likely related to the lower salinity of Tyro-T surface water compared to other river plume surface waters (Table 2). Thus, particles—carried in glacial meltwater transported from rivers into the fjord—are conduits for bacterial dispersal in these systems, shaping the river-to-fjord microbial community (Crump et al. 2012), and carbon cycling activities across this salinity gradient. The influence of riverine particles on microbial community composition, however, is limited in the inner and outer fjord, reflecting the combined effects of vertical particle export in the fjord and efficient particle degradation (Rysgaard and Sejr 2007).

Implications of findings in rapidly changing environments

Increased meltwater fluxes and fjord freshening (Sejr et al. 2017) may increase the proportions as well as the spatial and temporal persistence of freshwater, glacial, and terrestrial DOM constituents (Hood et al. 2015). Greater discharge could more effectively entrain and introduce particles into the fjord. Salinity-related changes in the composition of microbial communities in the fjord are likely, and may interact with changes in OM supply to alter the rates and spectra of enzymatic activities. Changes in these interwoven parameters (Fig. 8) may ultimately alter the retention and processing of glacially and terrestrially derived OM and autochthonous primary production, with consequences on the quantity and quality of OM available to downstream microbial communities (Hood and Berner 2009; Hood et al. 2009; Wassmann 2015). Quantifying

these microbiological and physicochemical changes, especially over longer timescales, will be necessary to better constrain future projections of carbon turnover in the coastal Arctic. Thus, projected increases in meltwater discharge into fjords have implications for microbially driven carbon cycling within the pan-Arctic, but these findings may also be more broadly applicable to other coastal systems, in transitions from freshwater to marine water.

References

Alderkamp, A. C., M. van Rijssel, and H. Bolhuis. 2007. Characterization of marine bacteria and the activity of their enzyme systems involved in degradation of the algal storage glucan laminarin. FEMS Microbiol. Ecol. **59**: 108–117. doi:10.1111/j.1574-6941.2006.00219.x

Amon, R. M. W., G. Budéus, and B. Meon. 2003. Dissolved organic carbon distribution and origin in the Nordic Seas: Exchanges with the Arctic Ocean and the North Atlantic. J. Geophys. Res. **108**: 1–17. doi:10.1029/2002JC001594

Arnosti, C. 2003. Fluorescent derivatization of polysaccharides and carbohydrate-containing biopolymers for measurement of enzyme activities in complex media. J. Chromatogr. B **793**: 181–191. doi:10.1016/S1570-0232(03)00375-1

Arnosti, C., Steen, A. D., Ziervogel, K., Ghobrial, S., and Jeffrey, W. H. 2011. Latitudinal gradients in degradation of marine dissolved organic carbon. PLoS One **6**: e28900.

Arnosti, C. 2015. Contrasting patterns of peptidase activities in seawater and sediments: An example from Arctic fjords of Svalbard. Mar. Chem. **168**: 151–156. doi:10.1016/j.marchem.2014.09.019

Balmonte, J. P., A. Teske, and C. Arnosti. 2018. Structure and function of high Arctic pelagic, particle-associated, and benthic bacterial communities. Environ. Microbiol. **20**: 2941–2954. doi:10.1111/1462-2920.14304

Balmonte, J. P., A. Buckley, A. Hoarfrost, S. Ghobrial, K. Ziervogel, A. Teske, and C. Arnosti. 2019. Community structural differences shape microbial responses to high molecular weight organic matter. Environ. Microbiol. **21**: 557–571. doi:10.1111/1462-2920.14485

Barman, T. E. 1969. Enzyme Handbook, p. 928. Springer Verlag, Berlin.

Bendtsen, J., J. Mortensen, and S. Rysgaard. 2014. Seasonal surface layer dynamics and sensitivity to runoff in a high Arctic fjord (Young Sound/Tyrolerfjord, 74°N). J. Geophys. Res. Oceans **119**: 6461–6478. doi:10.1002/2014JC010077

Benner, R. 2002. Chemical composition and reactivity, p. 59–90. *In* D. A. Hansell and C. A. Carlson [eds.], Biogeochemistry of marine dissolved organic matter. Elsevier.

Bhatia, M. P., S. B. Das, L. Xu, M. A. Charette, J. L. Wadham, and E. B. Kujawinski. 2013. Organic carbon export from the Greenland ice sheet. Geochim. Cosmochim. Acta **109**: 329–344. doi:10.1016/j.gca.2013.02.006

Bižić-Ionescu, M., and others. 2015. Comparison of bacterial communities on limnic versus coastal marine particles reveals profound differences in colonization. Environ. Microbiol. **17**: 3500–3514. doi:10.1111/1462-2920.12466

Bourgeois, S., P. Kerhervé, M. L. Calleja, G. Many, and N. Morata. 2016. Glacier inputs influence organic matter composition and prokaryotic distribution in a high Arctic fjord (Kongsfjorden, Svalbard). J. Mar. Syst. **164**: 112–127. doi:10.1016/j.jmarsys.2016.08.009

Cameron, K. A., and others. 2015. Diversity and potential sources of microbiota associated with snow on western portions of the Greenland Ice Sheet. Environ. Microbiol. **17**: 594–609. doi:10.1111/1462-2920.12446

Caporaso, J. G., and others. 2010. QIIME allows analysis of high-throughput community sequencing data. Nat. Methods **7**: 335–336. doi:10.1038/nmeth.f.303

Crump, B. C., E. V. Armbrust, and J. A. Baross. 1999. Phylogenetic analysis of particle-attached and free-living bacterial communities in the Columbia river, its estuary, and the adjacent coastal ocean. Appl. Environ. Microbiol. **65**: 3192–3204.

Crump, B. C., L. A. Amaral-Zettler, and G. W. Kling. 2012. Microbial diversity in arctic freshwaters is structured by inoculation of microbes from soils. ISME J. **6**: 1629–1639. doi:10.1038/ismej.2012.9

Cui, X., T. S. Bianchi, and C. Savage. 2017. Erosion of modern terrestrial organic matter as a major component of sediments in fjords. Geophys. Res. Lett. **44**: 1457–1465. doi:10.1002/2016GL072260

Cunha, M. A., M. A. Almeida, and F. Alcantara. 2000. Patterns of ectoenzymatic and heterotrophic bacterial activities along a salinity gradient in a shallow tidal estuary. Mar. Ecol. Prog. Ser. **204**: 1–12. doi:10.3354/meps204001

D'Ambrosio, L., K. Ziervogel, B. MacGregor, A. Teske, and C. Arnosti. 2014. Composition and enzymatic function of particle-associated and free-living bacteria: A coastal/offshore comparison. ISME J. **8**: 2167–2179. doi:10.1038/ismej.2014.67

Delong, E. F., D. G. Franks, and A. L. Alldredge. 1993. Phylogenetic diversity of aggregate-attached vs free-living marine bacterial assemblages. Limnol. Oceanogr. **38**: 924–934. doi:10.4319/lo.1993.38.5.0924

DeSantis, T. Z., and others. 2006. Greengemes, a chimera-checked 16S rRNA gene database and workbench compatible with ARB. Appl. Environ. Microbiol. **72**: 5069–5072. doi:10.1128/AEM.03006-05

Dittmar, T., B. Koch, N. Hertkorn, and G. Kattner. 2008. A simple and efficient method for the solid-phase extraction of dissolved organic matter (SPE-DOM) from seawater. Limnol. Oceanogr.: Methods **6**: 230–235. doi:10.4319/lom.2008.6.230

Dubnick, A., S. Kazemi, M. Sharp, J. Wadham, J. Hawkings, A. Beaton, and B. Lanoil. 2017. Hydrological controls on glacially exported microbial assemblages. J. Geophys. Res. Biogeosci. **122**: 1049–1061.doi:10.1002/2016JG003685

Eiler, A., and others. 2014. Productivity and salinity structuring of the microplankton revealed by comparative

freshwater metagenomics. Environ. Microbiol. **16**: 2682–2698. doi:10.1111/1462-2920.12301

Elifantz, H., L. A. Waidner, V. K. Michelou, M. T. Cottrell, and D. L. Kirchman. 2008. Diversity and abundance of glycosyl hydrolase family 5 in the North Atlantic Ocean. FEMS Microbiol. Ecol. **63**: 316–327. doi:10.1111/j.1574-6941.2007.00429.x

Fellman, J. B., R. G. M. Spencer, P. J. Hernes, R. T. Edwards, D. V. D'Amore, and E. Hood. 2010. The impact of glacier runoff on the biodegradability and biochemical composition of terrigenous dissolved organic matter in near-shore marine ecosystems. Mar. Chem. **121**: 112–122. doi:10.1016/j.marchem.2010.03.009

Fernandez-Gomez, B., and others. 2013. Ecology of marine Bacteroidetes: A comparative genomics approach. ISME J. **7**: 1026–1037. doi:10.1038/ismej.2012.169

Fortunato, C. S., and B. C. Crump. 2015. Microbial gene abundance and expression patterns across a river to ocean salinity gradient. PLoS One **10**: e0140578. doi:10.1371/journal.pone.0140578

Ghai, R., and others. 2011. Metagenomics of the water column in the pristine upper course of the Amazon River. PLoS One **6**: e23785. doi:10.1371/journal.pone.0023785

Glud, R. N., O. Holby, F. Hofmann, and D. E. Canfield. 1998. Benthic mineralization in Arctic sediments (Svalbard). Mar. Ecol. Prog. Ser. **173**: 237–251. doi:10.3354/meps173237

Gutiérrez, M. H., P. E. Galand, C. Moffat, and S. Pantoja. 2015. Melting glacier impacts community structure of Bacteria, Archaea and Fungi in a Chilean Patagonia fjord. Environ. Microbiol. **17**: 3882–3897. doi:10.1111/1462-2920.12872

Haas, B. J., and others. 2011. Chimeric 16S rRNA sequence formation and detection in sanger and 454-pyrosequenced PCR amplicons. Genome Res. **21**: 494–504. doi:10.1101/gr.112730.110

Hasler-Sheetal, H., L. Fragner, M. Holmer, and W. Weckwerth. 2015. Diurnal effects of anoxia on the metabolome of the seagrass *Zostera marina*. Metabolomics **11**: 1208–1218. doi:10.1007/s11306-015-0776-9

Hasler-Sheetal, H., M. C. N. Castorani, R. N. Glud, D. E. Canfield, and M. Holmer. 2016. Metabolomics reveals cryptic interactive effects of species interactions and environmental stress on nitrogen and sulfur metabolism in seagrass. Environ. Sci. Technol. **50**: 11602–11609. doi:10.1021/acs.est.6b04647

Hewson, I., and J. A. Fuhrman. 2004. Richness and diversity of bacterioplankton species along an estuarine gradient in Moreton Bay, Australia. Appl. Environ. Microbiol. **70**: 3425–3433. doi:10.1128/AEM.70.6.3425-3433.2004

Hollibaugh, J. T. 1988. Limitations of the [3H]thymidine method for estimating bacterial productivity due to thymidine metabolism. Mar. Ecol. Prog. Ser. **43**: 19–30. doi:10.3354/meps043019

Hood, E., and D. Scott. 2008. Riverine organic matter and nutrients in southeast Alaska affected by glacial coverage. Nat. Geosci. **1**: 583–587. doi:10.1038/ngeo280

Hood, E., and L. Berner. 2009. The effect of changing glacial coverage on the physical and biogeochemical properties of coastal streams in southeastern Alaska. J. Geophys. Res. **114**: G03001.

Hood, E., and others. 2009. Glaciers as a source of ancient and labile organic matter to the marine environment. Nature **462**: 1044–1047. doi:10.1038/nature08580

Hood, E., T.J. Battin, J. Fellman, S. O'Neel and R.G.M Spencer. 2015. Storage and release of organic carbon from glaciers and ice sheets. Nat. Geosci. **8**: 91–96.

Hoppe, H. G. 1983. Significance of exoenzymatic activities in the ecology of brackish water: Measurements by means of methylumbelliferyl-substrates. Mar. Ecol. Prog. Ser. **11**: 299–308. doi:10.3354/meps011299

Jain, A., and others. 2019. Biochemical composition of particles shape particle-attached bacterial community structure in a high Arctic fjord. Ecol. Indic. **102**: 581–592. doi:10.1016/j.ecolind.2019.03.015

Lawson, E. C., and others. 2014. Greenland Ice Sheet exports labile organic carbon to the Arctic oceans. Biogeosciences **11**: 4015–4028. doi:10.5194/bg-11-4015-2014

Marie, D., C. P. D. Brussaard, R. Thyrhaug, G. Bratbak, and D. Vaulot. 1999. Enumeration of marine viruses in culture and natural samples by flow cytometry. Appl. Environ. Microbiol. **65**: 45–52.

McMurdie, P. J., and S. Holmes. 2013. phyloseq: An R package for reproducible interactive analysis and graphics of microbiome census data. PLoS One **8**: e61217. doi:10.1371/journal.pone.0061217

Murrell, M. C., J. T. Hollibaugh, M. W. Silver, and P. S. Wong. 1999. Bacterioplankton dynamics in northern San Francisco Bay: Role of particle association and seasonal freshwater flow. Limnol. Oceanogr. **44**: 295–308. doi:10.4319/lo.1999.44.2.0295

Neumann, A. M., and others. 2015. Different utilization of alginate and other algal polysaccharides by marine *Alteromonas macleodii* ecotypes. Environ. Microbiol. **17**: 3857–3868. doi:10.1111/1462-2920.12862

Obayashi, Y., and Suzuki, S. 2005. Proteolytic enzymes in coastal surface seawater: significant activity of endopeptidases and exopeptidases. Limnol. Oceanogr. **50**: 722–726.

Oksanen J., and others. 2013. vegan: Community ecology package. R package version 2.0–10. Available from http://vegan.r-forge.r-project.org/

Opsahl, S., and R. Benner. 1999. Characterization of carbohydrates during early diagenesis of five vascular plant tissues. Org. Geochem. **30**: 83–94. doi:10.1016/S0146-6380(98)00195-8

Ortega-Retuerta, E., F. Joux, W. H. Jeffrey, and J. F. Ghiglione. 2013. Spatial variability of particle-attached and free-living bacterial diversity in surface waters from the Mackenzie River to the Beaufort Sea (Canadian Arctic). Biogeosciences **10**: 2747–2759. doi:10.5194/bg-10-2747-2013

Osterholz, H., T. Dittmar, and J. Niggemann. 2014. Molecular evidence for rapid dissolved organic matter turnover in Arctic fjords. Mar. Chem. **160**: 1–10. doi:10.1016/j.marchem.2014.01.002

Osterholz, H., and others. 2016. Deciphering associations between dissolved organic molecules and bacterial communities in a pelagic marine system. ISME J. **10**: 1717–1730. doi:10.1038/ismej.2015.231

Overeem, I., and others. 2017. Substantial export of suspended sediment to the global oceans from glacial erosion in Greenland. Nat. Geosci. **10**: 859–863. doi:10.1038/ngeo3046

Painter, T. J. 1983. Algal polysaccharides, p. 195–285. *In* G. O. Aspinall [ed.], The polysaccharides, v. **2**. Academic Press.

Paulsen, M. L., and others. 2017. Carbon bioavailability in a high Arctic fjord influenced by glacial meltwater, NE Greenland. Front. Mar. Sci. **4**: 176. doi:10.3389/fmars.2017.00176

Paulsen, M. L., and others. 2018. Biological transformation of Arctic dissolved organic matter in a NE Greenland fjord. Limnol. Oceanogr. **64**: 1014–1033. doi:10.1002/lno.11091

Riemann, B., J. Fuhrman, and F. Azam. 1982. Bacterial secondary production in freshwater measured by ^{3}H-thymidine incorporation method. Microb. Ecol. **8**: 101–113. doi:10.1007/BF02010444

Ruiz-González, C., J. P. Niño-Garcia, J.-F. Lapierre, and P. A. del Giorgio. 2015. The quality of organic matter shapes the functional biogeography of bacterioplankton across boreal freshwater ecosystems. Glob. Ecol. Biogeogr. **24**: 10487–11498.

Rysgaard, S., and M. K. Sejr. 2007. Vertical flux of particulate organic matter in a High Arctic fjord: Relative importance of terrestrial and marine sources, p. 110–119. *In* S. Rysgaard and R. N. Glud [eds.], Carbon cycling in Arctic marine ecosystems: Case study Young Sound. Meddr. Grønland, Bioscience, Museum Tusculanum Press, University of Copenhagen v. **58**.

Sala, M. M., J. M. Arrieta, J. A. Boras, C. M. Duarte, and D. Vaqué. 2010. The impact of ice melting in natural communities. FEMS Microbiol. Ecol. **62**: 161–170.

Schmidt, M. L., J. D. White, and V. J. Denef. 2016. Phylogenetic conservation of freshwater lake habitat preference varies between abundant bacterioplankton phyla. Environ. Microbiol. **18**: 1212–1226. doi:10.1111/1462-2920.13143

Sejr, M., and others. 2017. Evidence of local and regional freshening of Northeast Greenland coastal waters. Sci. Rep. **7**: 13183.

Simon, H. M., M. W. Smith, and L. Herfort. 2014. Metagenomic insights into particles and their associated microbiota in a coastal margin ecosystem. Front. Microbiol. **5**: 1–10. doi:10.3389/fmicb.2014.00466

Smith, R. E. H., and P. Clement. 1990. Heterotrophic activity and bacterial productivity in assemblages of microbes from sea ice in the high Arctic. **10**: 351–357.

Smith, R. W., T. S. Bianchi, M. Allison, C. Savage, and V. Galy. 2015. High rates of organic carbon burial in fjord sediments globally. Nat. Geosci. **8**: 450–453. doi:10.1038/ngeo2421

Sørensen, H. L., and others. 2015. Seasonal carbon cycling in a Greenlandic fjord: An integrated pelagic benthic study. Mar. Ecol. Prog. Ser. **539**: 1–17. doi:10.3354/meps11503

Sperling, M., and others. 2013. Effect of elevated CO_2 on the dynamics of particle-attached and free-living bacterioplankton communities in an Arctic fjord. Biogeosciences **10**: 181–191. doi:10.5194/bg-10-181-2013

Steen, A. D., and C. Arnosti. 2013. Extracellular peptidase and carbohydrate hydrolase activities in an Arctic fjord (Smeerenburgfjord, Svalbard). Aquat. Microb. Ecol. **69**: 93–99. doi:10.3354/ame01625

Steen, A. D., Vazin, J. P., Hagen, S. M., Mulligan, K. H., and Wilhelm, S. W. 2015. Substrate-specificity of aquatic extracellular peptidases assessed by competitive inhibition assays using synthetic substrates. Aquat. Microb. Ecol. **75**: 271–281.

Stepanauskas, R., H. Edling, and L. J. Tranvik. 1999. Differential dissolved organic nitrogen availability and bacterial aminopeptidase activity in limnic and marine waters. Microb. Ecol. **38**: 264–272. doi:10.1007/s002489900176

Stibal, M., E. C. Lawson, G. P. Lis, K. M. Mak, J. L. Wadham, and A. M. Anesio. 2010. Organic matter content and quality in supraglacial debris across the ablation zone of the Greenland ice sheet. Ann. Glaciol. **51**: 1–8. doi:10.3189/172756411795931958

Stibal, M., M. Sabacka, and J. Zarsky. 2012. Biological processes on glacier and ice sheet surfaces. Nat. Geosci. **5**: 771–774. doi:10.1038/ngeo1611

Teske, A., A. Durbin, K. Ziervogel, C. Cox, and C. Arnosti. 2011. Microbial community composition and function in permanently cold seawater and sediments from an Arctic fjord of Svalbard. Appl. Environ. Microbiol. **77**: 2008–2018. doi:10.1128/AEM.01507-10

Wassmann, P. 2015. Overarching perspectives of contemporary and future ecosystems in the Arctic Ocean. Prog. Oceanogr. **139**: 1–12. doi:10.1016/j.pocean.2015.08.004

Wetzel, R. G. 1991. Extracellular enzymatic interactions in aquatic ecosystems: Storage, redistribution, and interspecific communication, p. 6-26. *In* R. J. Chróst [ed.], Extracellular enzymes in aquatic ecosystems. Springer-Verlag.

Zeng, Y., T. Zheng, and H. Li. 2009. Community composition of the marine bacterioplankton in Kongsfjorden (Spitsbergen) as revealed by 16S rRNA gene analysis. Polar Biol. **32**: 1447–1460. doi:10.1007/s00300-009-0641-2

Acknowledgments

We thank Egon and Charlotte Frandsen, Karl Attard, Johnna Holding, and Achim Randelhoff for their field and lab support, scientific advice, and camaraderie. We additionally thank Sherif Ghobrial and Karylle Abella for their assistance with sample processing, as well as Jake Reardon for editing the manuscript. JPB and CA were supported by NSF (OCE-1332881 and OCE-1736772 to CA), and JPB was additionally funded by a UNC Dissertation Completion Fellowship. RNG and MM were supported by European Union's Horizon 2020 Research and Innovation Program (Grant agreement 669947; HADES-ERC) and the Danish National Research Council (FNU 0602-02276B and 7014-00078). This work was also partially funded by a

Deep Carbon Observatory Diversity Grant from the American Geosciences Institute awarded to JPB.

Conflict of Interest

None declared.

Submitted 19 April 2018
Revised 12 August 2018; 24 March 2019 and 11 June 2019
Accepted 26 June 2019

Associate editor: Peter Hernes